TEVATRON SM SCALAR BOSON RESULTS - UPDATED INPUTS AND INDIVIDUAL COMBINATIONS

L. ZIVKOVIC
LPNHE, Paris Univ VI & VII, CNRS/IN2P3, France

The CDF and D0 experiments at the Tevatron $p\bar{p}$ Collider were collecting data between 2002 and 2011. During that time, the extensive search for the standard model Higgs boson was performed. Every accessible decay mode was investigated. Results from the searches for the standard model Higgs boson with the final dataset will be presented for individual channels, as well as combined results from the CDF and D0 experiments individually.

1 Introduction

The standard model (SM) Higgs boson was introduced to explain electroweak symmetry breaking.[1–5] The search for the Higgs boson was a central part of the D0 and CDF Collaborations physics program for many years. Recently both experiments finalized their searches, and prepared final publications.[6–29] In section 2 we will present overview of the Higgs boson search analyses, and describe the most important channels $H \to W^+W^-$ (section 2.1) and $VH \to Vb\bar{b}$ (section 2.2). We will describe validation of the searches in section 3, and present results in section 4.

2 Overview of the searches

A list of the analyses used in this combination is given in Table 1. We summarize the analyses, grouping them according to the Higgs boson decay mode to which the analysis is most sensitive. All D0 (CDF) analyses use up to 9.7 (10) fb^{-1} of data collected between April of 2002 September of 2011.

2.1 Search for the $H \to WW$

The $H \to W^+W^-$ is the most sensitive search channel for the Higgs boson mass, M_H, above ~ 135 GeV. We divided final states according to the decay modes of the W boson pairs, where we included $H \to W^+W^- \to \ell^+\nu\ell^-\bar{\nu}$, $H \to W^+W^- \to \ell\nu jj$, and $H+X \to WW \to \mu^{\pm}\tau_h^{\mp}+ \leq 1$ jet final states. Searches are also divided according to the production mode of the Higgs boson into events with various jet multiplicities, and we also included searches for the final states with at least three leptons.

The $H \to W^+W^- \to \ell^+\nu\ell^-\bar{\nu}$ is the most sensitive final state among $H \to W^+W^-$ channels. It is characterized by the two isolated high transverse momentum, p_T, leptons and high missing transverse energy, $\not\!\!E_T$. At both experiments, D0 and CDF, lepton identification significantly

Table 1: Overview of the search channels for the D0 and CDF experiments.

Channel ($V = W, Z$ and $\ell = e, \mu$)	Luminosity (fb^{-1})	M_H (GeV)
$WH \to \ell\nu b\bar{b}$[6,7]	9.7	90–150
$ZH \to \ell\ell b\bar{b}$[8,9]	9.7	90–150
$ZH \to \nu\bar{\nu}b\bar{b}$[10]	9.5	100–150
$H \to W^+W^- \to \ell^+\nu\ell^-\bar{\nu}$[11]	9.7	100–200
$H + X \to WW \to \mu^\pm\tau_h^\mp + \leq 1$ jet[12]	7.3	155–200
$H \to W^+W^- \to \ell\nu q'\bar{q}$[7]	9.7	100–200
$VH \to ee\mu/\mu\mu e{+}X$[13]	9.7	100–200
$VH \to e^\pm\mu^\pm{+}X$[13]	9.7	100–200
$VH \to \ell\nu q'\bar{q}q'\bar{q}$[7]	9.7	100–200
$VH \to \tau_h\tau_h\mu + X$[13]	8.6	100–150
$H + X \to \ell\tau_h jj$[14]	9.7	105–150
$H \to \gamma\gamma$[15]	9.7	100–150
CDF		
$WH \to \ell\nu b\bar{b}$[18]	9.45	90–150
$ZH \to \ell\ell b\bar{b}$[19]	9.45	90–150
$ZH \to \nu\bar{\nu}b\bar{b}$[20,21]	9.45	90–150
$H \to W^+W^- \to \ell^+\nu\ell^-\bar{\nu}$[22]	9.7	110–200
$H \to WW \to e\tau_h\mu\tau_h$[22]	9.7	130–200
$VH \to ee\mu/\mu\mu e{+}X$[22]	9.7	110–200
$H \to ZZ \to llll$[23]	9.7	120–200
$H \to \tau\tau$[24]	6.0	100–150
$VH \to jjb\bar{b}$[25]	9.45	100–150
$H \to \gamma\gamma$[26]	10.0	100–150
$t\bar{t}H \to WWb\bar{b}b\bar{b}$[27]	9.45	100–150

improved over the years to allow for more efficient selection. We used multiple multivariate analyses (MVA) in the Higgs boson searches to separate signal from SM backgrounds. To reduce the most dominant background process, $Z(\to \ell\ell) + \text{jets}$, we use a dedicated MVA at the D0 experiment (Fig. 1 (left)). Depending on the M_H we select events that pass a certain threshold. Then we divide these events based on the output of the MVA that is trained to separate diboson WW backgrounds from other backgrounds into WW-depleted and WW-enriched regions. Another MVA used to separate Higgs boson signal from all backgrounds then serves as a final discriminant to set limits on the production cross section as shown in Fig. 1 (middle) WW-depleted and (right) WW-enriched regions.

Figure 2 shows 95% C.L. upper limit on the Higgs boson production cross section as a ratio to the SM cross section, σ_{SM}, as a function of the M_H for (left) CDF and (right) D0 Collaboration. The CDF experiment excludes (expects to exclude) the Higgs boson with $149 < M_H < 172$ GeV ($153 < M_H < 175$ GeV), while the D0 experiment excludes (expects to exclude) the Higgs boson with $157 < M_H < 178$ GeV ($155 < M_H < 175$ GeV). At $M_H = 125$ GeV the expected (observed) limit is $3.1 \times \sigma_{SM}$ ($2.9 \times \sigma_{SM}$) at CDF, and $3.1 \times \sigma_{SM}$ ($3.1 \times \sigma_{SM}$) at D0.

2.2 Search for the $H \to b\bar{b}$

Due to the overwhelming backgrounds from the multijet productions, a search for the Higgs boson in the final state with the two b-quarks is performed in the associated production with a vector boson V ($V = W, Z$). The search is divided according to the decay of the associated

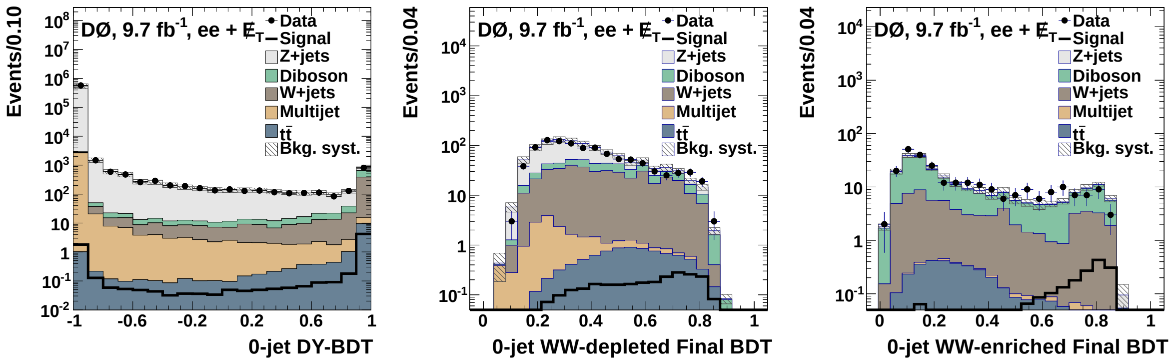

Figure 1: Various MVA outputs in D0 $H \to W^+W^-$ analysis: (left) against $Z+$jets backgrounds, and the final MVA for (middle) WW-depleted and (right) WW-enriched regions.

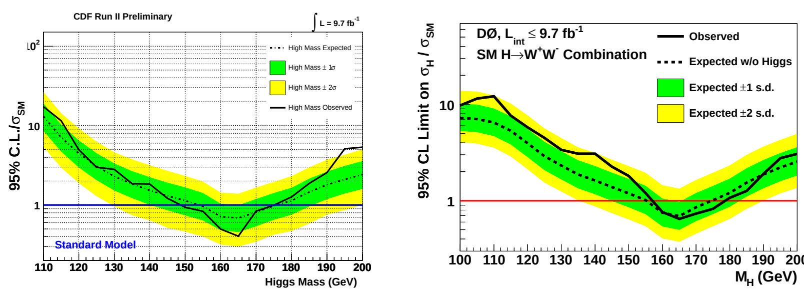

Figure 2: Expected (median) and observed ratios for the upper limits of the cross section σ_H at 95% C.L. relative to the SM values for the combined $WH/ZH/H, H \to W^+W^-$ analyses for the range $100 \leq M_H \leq 200$ GeV for (left) CDF and (right) D0 experiments.

vector boson into: (a) $ZH \to \ell\ell b\bar{b}$, (b) $WH \to \ell\nu b\bar{b}$, and (c) $ZH \to \nu\bar{\nu}b\bar{b}$. One of the main ingredients of the search in these final states is an identification of the jets originating from the b-quarks, i.e. b-tagging. Both the CDF and D0 collaborations use MVA for b-tagging which improved efficiency significantly. The most recent optimization of the b-tagging algorithm, called HOBIT, at the CDF experiment led to the efficiency of the 54% (59%) for the mistag rate of 1.4% (2.9%) for the tight (loose) operating point. This represents $\sim$ 14% improvements over the previous b-tagging algorithm.

The CDF Collabration recently updated $ZH \to \nu\bar{\nu}b\bar{b}$ analysis using HOBIT algorithm, which led to the improvement in sensitivity at $M_H = 125$ GeV of 8%, and about 14% over all mass region investigated. This analysis uses a dedicated MVA to reject dominant multijet backgrounds (Fig. 1 (left)). Figure 3 (right) shows the final MVA used to obtain final result.

3 Validation of the results

We measure the cross sections of SM processes with similar characteristics as the Higgs boson signal to validate our procedures and results. At the D0 experiment, we measure the cross section of the WW process and we obtained $\sigma = (1.02 \pm 0.06) \times \sigma_{SM}$. Both the D0 and CDF Collaborations measure the cross section of the $VZ \to Vb\bar{b}$ processes to be $\sigma = (0.73 \pm 0.32) \times \sigma_{SM}$ (D0) and $\sigma = (0.59 \pm 0.30) \times \sigma_{SM}$ (CDF).

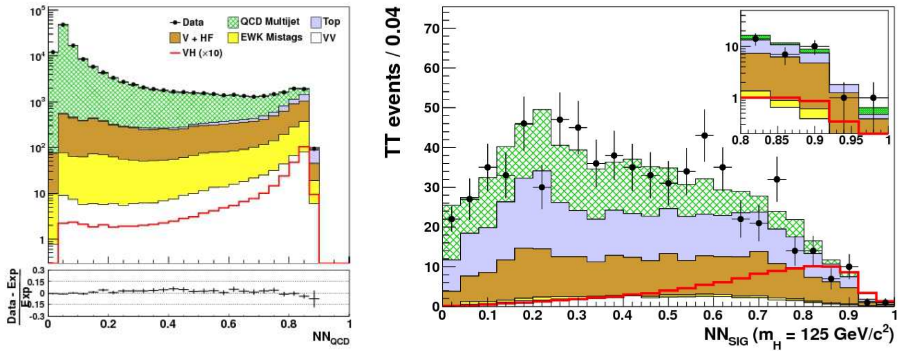

Figure 3: Expected (median) and observed ratios for the upper limits of the cross section σ_H at 95% C.L. relative to the SM values for the combined $WH/ZH/H, H \to W^+W^-$ analyses for the range $100 \leq M_H \leq 200$ GeV for (left) CDF and (right) D0 experiments.

4 Combined results from D0 and CDF experiments

To estimate the sensitivity of the search at the D0 experiment we use log-likelihood ratio (LLR) test statistic for the signal-plus-background ($s+b$) and background-only (b) hypotheses, defined as $\mathrm{LLR} = -2\ln(L_{s+b}/L_b)$, and L_{hy} is the likelihood function for the hypothesis hy as shown in Fig. 4 (left). Included in this figure are the median LLR values expected for the $s+b$ hypothesis (LLR_{s+b}), b hypothesis (LLR_b), and the results observed in data ($\mathrm{LLR}_{\mathrm{obs}}$). The shaded bands represent the ± 1 and ± 2 standard deviations (s.d.) departures for LLR_b. These distributions can be interpreted as follows:

- The separation between LLR_b and LLR_{s+b} provides a measure of the discriminating power of the search, and illustrates the effectiveness of the analysis to separate the $s+b$ and b hypotheses.
- The width of the LLR_b distribution (shown here as ± 1 and ± 2 s.d. bands) provides an estimate of the sensitivity of the analysis to a signal-like background fluctuation in the data, taking the systematic uncertainties into account. For example, the sensitivity is limited when a 1 s.d. background fluctuation is large compared to the difference between the $s+b$ and b expectations.
- The value of $\mathrm{LLR}_{\mathrm{obs}}$ relative to LLR_{s+b} and LLR_b indicates whether the data distribution appears to be more $s+b$-like or b-like. The significance of any departures of $\mathrm{LLR}_{\mathrm{obs}}$ from LLR_b can be evaluated through the width of the LLR_b distribution.

We present in Fig. 4 (middle) (D0) and (right) (CDF) local p-values for b hypothesis, which provide information about the consistency with the observed data. Values greater than about 50% mean that a hypothesis is consistent with the data, while small values mean it is inconsistent. We obtain that background is inconsistent with the data at the level of 1.7 (2.0) s.d. for D0 (CDF) experiments at $M_H = 125$ GeV.

To estimate how big Higgs boson signal can fit the excess in data we calculate signal strength (Fig. 5) and obtain that it is consistent with SM within one s.d. We also present signal strength in each decay mode. Results are presented in Table 2 and in Fig. 6.

5 Summary

In summary, we presented recent results from the D0 and CDF Collaboration in the search for the Higgs boson. Both Collaborations implemented many improvements over the years which

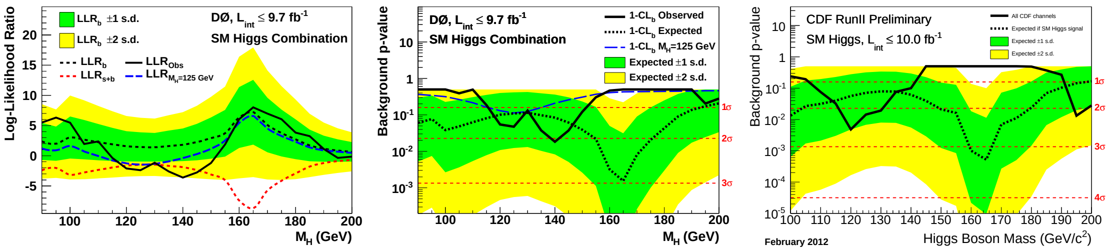

Figure 4: The (left) LLR distribution form the D0 experiment, and p-value for the (middle) D0 and (right) CDF experiments.

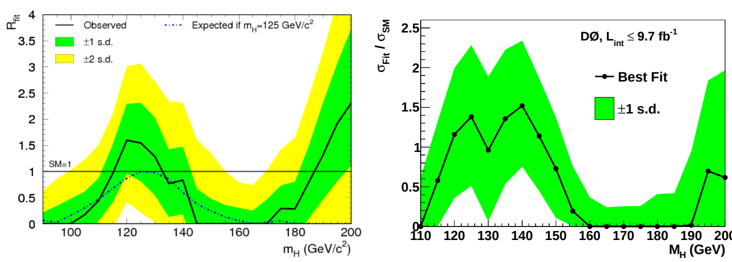

Figure 5: Signal strength for (left) CDF and (right) D0 experiments.

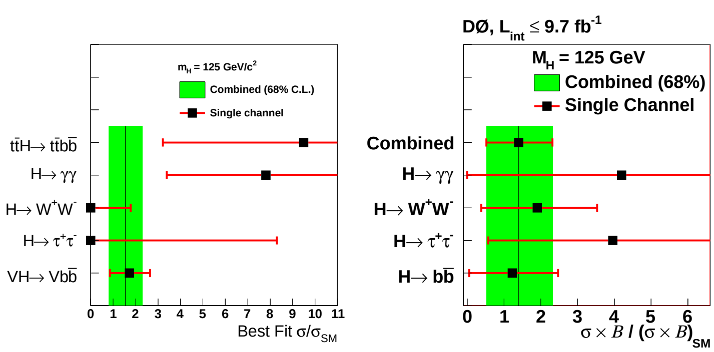

Figure 6: Signal strength for various decay modes for (left) CDF and (right) D0 experiments.

Table 2: Signal strength for various decay modes for CDF and D0 experiments..

	DØ	CDF
Combination	$1.40^{+0.92}_{-0.88}$	$1.54^{+0.77}_{-0.73}$
$H \to \gamma\gamma$	$4.20^{+4.60}_{-4.20}$	$7.81^{+4.61}_{-4.42}$
$H \to \tau^+\tau^-$	$3.96^{+4.11}_{-4.38}$	$0.00^{+8.44}_{-0.00}$
$H \to W^+W^-$	$1.90^{+1.63}_{-1.52}$	$0.00^{+1.78}_{-0.00}$
$VH \to Vb\bar{b}$	$1.23^{+1.24}_{-1.17}$	$1.72^{+0.92}_{-0.87}$
$t\bar{t}H \to t\bar{t}b\bar{b}$	N/A	$9.49^{+6.60}_{-6.28}$

led to the sensitivity of about $1 \times \sigma_{SM}$ for $M_H < 185$ when combined.[30] Excess of about 2 s.d. between 120 and 135 GeV in both experiments is observed, consistent with the SM scalar boson recently discovered at LHC.

Acknowledgments

We thank the staffs at Fermilab and collaborating institutions, and acknowledge support from the DOE and NSF (USA); CEA and CNRS/IN2P3 (France); MON, NRC KI and RFBR (Russia); CNPq, FAPERJ, FAPESP and FUNDUNESP (Brazil); DAE and DST (India); Colciencias (Colombia); CONACyT (Mexico); NRF (Korea); FOM (The Netherlands); STFC and the Royal Society (United Kingdom); MSMT and GACR (Czech Republic); BMBF and DFG (Germany); SFI (Ireland); The Swedish Research Council (Sweden); and CAS and CNSF (China).

References

1. P. W. Higgs, *Phys. Lett.*, 12, 132, (1964).
2. P. W. Higgs, *Phys. Rev. Lett.*, 13, 508, (1964).
3. P. W. Higgs, *Phys. Rev.*, 145, 1156, (1966).
4. F. Englert and R. Brout, *Phys. Rev. Lett.*, 13, 321, (1964).
5. G. S. Guralnik, C. R. Hagen, and T. W. B. Kibble, *Phys. Rev. Lett.*, 13, 585, (1964).
6. V. M. Abazov *et al.*, [D0 Collaboration], *Phys. Rev. Lett.*, **109**, 121804, (2012).
7. V. M. Abazov *et al.*, [D0 Collaboration], arXiv:1301.6122, (2013), accepted by Phys. Rev. D.
8. V. M. Abazov *et al.*, [D0 Collaboration], *Phys. Rev. Lett.*, **109**, 121803, (2012).
9. Paper in preparation.
10. V. M. Abazov *et al.*, [D0 Collaboration], *Phys. Lett.*, B **716**, 285, (2012).
11. V. M. Abazov *et al.*, [D0 Collaboration], arXiv:1301.1243, (2013), accepted by Phys. Rev. D.
12. V. M. Abazov *et al.*, [D0 Collaboration], *Phys. Lett.*, B **714**, 237, (2012).
13. V. M. Abazov *et al.*, [D0 Collaboration], arXiv:1302.5723, (2013), accepted by Phys. Rev. D.
14. V. M. Abazov *et al.*, [D0 Collaboration], arXiv:1211.6993, (2012), accepted by Phys. Rev. D.
15. V. M. Abazov *et al.*, [D0 Collaboration], arXiv:1301.5358, (2013), accepted by Phys. Rev. D.
16. V. M. Abazov *et al.*, [D0 Collaboration], *Phys. Rev. Lett.*, 109, 121802, (2012).

17. V. M. Abazov *et al.*, [D0 Collaboration], arXiv:1303.0823, (2013), accepted by Phys. Rev. D.
18. T. Aaltonen *et al.*, [CDF Collaboration], *Phys. Rev. Lett.*, **109**, 111804, (2012).
19. T. Aaltonen *et al.*, [CDF Collaboration], *Phys. Rev. Lett.*, **109**, 111803, (2012).
20. T. Aaltonen *et al.*, [CDF Collaboration], *Phys. Rev. Lett.*, **109**, 111805, (2012).
21. T. Aaltonen *et al.*, [CDF Collaboration], arXiv:1301.4440, (2013), accepted by Phys. Rev. D.
22. T. Aaltonen *et al.*, [CDF Collaboration], (2013), FERMILAB-PUB-13-029-E, for submission to PRD.
23. T. Aaltonen *et al.*, [CDF Collaboration], *Phys. Rev.*, D **86**, 072012, (2012).
24. T. Aaltonen *et al.*, [CDF Collaboration], *Phys. Rev. Lett.*, **108**, 181804, (2012).
25. T. Aaltonen *et al.*, [CDF Collaboration], *J. High Energy Phys.*, **1302**, 004, (2013).
26. T. Aaltonen *et al.*, [CDF Collaboration], *Phys. Lett.*, B **717**, 173, (2012).
27. T. Aaltonen *et al.*, [CDF Collaboration], *Phys. Rev. Lett.*, **109**, 181802, (2012).
28. T. Aaltonen *et al.*, [CDF Collaboration], *Phys.Rev.Lett.*, 109, 111802, (2012).
29. T. Aaltonen *et al.*, [CDF Collaboration], arXiv:1301.6668, (2013), accepted by Phys. Rev. D.
30. W. Yao, *Tevatron combination and higgs boson properties.* In this proceedings, (2013).